

DETAILED DYNAMIC MODELING OF AUTO-THERMAL GASOLINE FUEL-PROCESSORS

¹Böhme, Thomas R. *, ¹Onder, Christopher, ¹Guzzella, Lino
¹Measurement and Control Laboratory, ETH Zurich, Switzerland

KEYWORDS – Fuel processing, Gasoline reforming, Dynamic modeling, Transient operation, Reaction kinetics

ABSTRACT – The dynamic performance of fuel-processors is critical for their automotive on-board application. In order to keep additional storage capacities to a minimum, a fast tracking of the hydrogen demand of the fuel-cell is essential. However, so far, little is known about the dynamic behavior of reformer systems. In order to gain a deeper understanding of the dynamic behavior, a detailed dynamic model for an experimental auto-thermal gasoline reformer has been developed. The reformer, a monolithic catalytic reactor, is modeled as a system of one-dimensional partial differential equations for mass and energy transport coupled to a simplified surface reaction mechanism. Surface occupancies of intermediate species are treated as dynamic states in order to allow an assessment of the importance of surface dynamics for the system behavior. Parameters for the reaction kinetics are obtained either from literature or estimated from measurements performed on a dynamic fuel-processor test bench built at our lab. Model versus experiment comparisons are presented for steady-state as well as for dynamic input step changes, indicating a good model agreement. For the input steps, it is shown that the non-ideal behavior of the test bench's reactant supply strongly influences the transient hydrogen output and simulations results for an ideal input steps are presented.

TECHICAL PAPER – The lack of a hydrogen infrastructure and high-density on-board storage systems are some of the major obstacles preventing the wide-scale introduction of fuel cells in automotive applications. Liquid fuel processors are considered to present a feasible solution to overcome these limitations. Fuel processors use a catalytic process to convert hydrocarbons into a hydrogen rich reformat gas which can be used to power fuel cells. However, for the direct use of fuel processors in vehicle propulsion systems, a fast tracking of the hydrogen demanded by the fuel cell is required. In order to minimize additional storage systems, response times in the range of a second or faster are desired. Currently, the fast dynamic behavior of fuel processors is little understood. Here, a mathematical model can help to understand the dynamic behavior of the system and facilitate the development of suitable control techniques.

To date, only few dynamical models of gasoline reformers have been presented (1-3). In all of them, the reaction kinetics is solely based on the gas phase species concentrations. This implies the assumption of a negligible dynamics of the catalyst surface. To our knowledge, no investigation about the validity of this assumption has been done to date. It is known that e.g. three way catalytic converters for exhaust gas aftertreatment show dynamic phenomena due to catalyst surface occupancies with time constants well in the seconds range (4). While the catalysts used for such converters are similar to the ones used in fuel processing, the input concentrations, conversion rates, and temperature profiles of both processes differ greatly. Therefore, the presence of dynamic phenomena in catalytic converters cannot give an indication whether such phenomena are of importance for fuel processing as well. The model

presented in this work includes dynamic effects of surface species. This will allow an evaluation, whether the catalytic surface does contribute significantly to the dynamics or not.

In the following, the experimental setup used to perform the measurements presented in this paper will be presented briefly. Then, the basic structure of the model and the reaction scheme used will be presented. Hereby, we will focus on the model of the gasoline oxidation and reforming and propose a two-step mechanism resulting in good agreement with measurements. In the next section, the numerical solver and parameter estimation technique used will be briefly discussed. Then, steady state comparisons for a wide range of operating conditions are presented as model validation. Following the steady-state validation, measurement vs. model result for input step changes will be presented and the influence of the input dynamics will be discussed.

FUEL PROCESSOR TEST BENCH

Measurements presented in this paper have been performed on a dynamic fuel processor test bench built in our lab. The test bench has a maximum input stream of gasoline equivalent to 4kW_{th} based on lower heating value. The fuel used is a sulfur free, 95 octane gasoline provided by Tamoil. The reformer consists of a tubular reactor with three metallic monoliths. The monoliths are coated with a precious metal based catalyst. The monoliths have a diameter of 25mm and a length of ca. 40mm each. In order to prevent gas bypass around the monoliths, they are insulated against the wall by a ceramic mat. Gas analysis is performed using a Pfeiffer OmniStar mass spectrometer. This allows for fast transient measurements with sampling frequencies of approximately one second. In order to increase the reliability of CO measurement, nitrogen in the feed was substituted by Argon. This did not result in significant changes of the system behavior. The reactants are heated respectively evaporated separately in electrical heaters and mixed shortly before entering the reactor. The time constants of the reactant supplies are roughly one second, allowing for fast transient excitations.

FUEL PROCESSOR MODEL

The aim of this model is to provide a good representation of the most important dynamic aspects of a gasoline fuel processor. The model is not expected to provide a complete and exact quantitative representation, as this is beyond feasible limits for such complex systems. However, as it is not yet clear whether the catalyst surface dynamics play a relevant role, the surface occupancies have been assumed dynamic rather than using a quasi-steady-state approach. This will allow investigating whether the influence is substantial or not.

The fuel processor is modeled as a system of one-dimensional partial differential equations along the axial reactor coordinate. Temperature and concentration gradients in radial direction are neglected. While the experimental results show temperature deviations of up to 50K between the reactor middle and near the wall, this assumption has been made to keep the computational demand of the model within feasible limits. With this assumption, the fuel-processor model can be reduced to the model of a single catalyst channel coupled to the reactor wall.

Mass Balances

For the mass balances, the channel is divided in three phases: an inner gas phase, a stagnant gas film close to and including the washcoat and the active catalyst surface itself. All three

phases are modeled as dynamic with their concentrations dependent on axial location. In the inner gas phase, mass is transferred by axial convection and diffusion. In the stagnant film near the coating, which includes the washcoat pores, transport processes are assumed to be purely diffusive. The mass transfer between the inner gas phase and the stagnant film is modeled using an effective diffusion coefficient determined from a constant Sherwood number $Sh = 2r_{channel} D_{j,eff}^{gas,wc} / D_j = 4$. This value represents the average between the asymptotical values for the constant wall temperature and constant wall flux case (5).

Weight fractions have been chosen as state variables for the gas phase and the stagnant film. In systems where the mole number changes significantly, this provides a more convenient basis. Gas dynamics have been neglected by assuming a constant mass flow and pressure along the reactor coordinate. This leads to small dynamic errors in the mass balances when the total holdup in the reactor changes over time. However, compared to the convective flows, the flows due to change of holdup are small. Given these assumptions, the mass balances are given by

Mass balances gas phase:

$$\varepsilon_{gas} \rho_{gas} \frac{\partial w_j^{gas}}{\partial t} = \overbrace{\varepsilon_g D_{j,eff}^{gas} \frac{\partial^2 w_j^{gas}}{\partial z^2}}^{\text{axial diffusion}} - \overbrace{\dot{m} \frac{\partial w_j^{gas}}{\partial z}}^{\text{convection}} - \overbrace{J_j^{gas,wc} + w_j^{gas} \sum_i^{NC} J_i^{gas,wc}}^{\text{diffusion gas} \leftrightarrow \text{washcoat}} \quad (1.1)$$

Mass balances stagnant film including washcoat:

$$\varepsilon_{wc} \rho_{wc} \frac{\partial w_j^{wc}}{\partial t} = \underbrace{D_{j,eff}^{wc} \frac{\partial^2 w_j^{wc}}{\partial z^2}}_{\text{axial diffusion}} + \underbrace{J_j^{g,w} - w_j^{wc} \sum_{i=1}^{NC} J_i^{gas,wc}}_{\text{diffusion gas} \leftrightarrow \text{washcoat}} + \underbrace{M_j \sum_{i=1}^{NR} \nu_{j,i} r_i - w_j^{wc} \sum_{k=1}^{NC} M_k \sum_{i=1}^{NR} \nu_{k,i} r_i}_{\text{reaction source term}} \quad (1.2)$$

Mass balances catalyst surface:

$$C_{nm} \frac{\partial \theta_j}{\partial t} = \underbrace{D_{j,eff}^{nm} \frac{\partial^2 \theta_j}{\partial z^2}}_{\text{axial diffusion}} + \underbrace{\sum_i^{NR} \nu_{j,i} r_{reac,i}}_{\text{reaction source term}}, \quad (1.3)$$

with the diffusive flux between the gas and the washcoat given by

$$J_{gas,wc} = D_{j,eff}^{gas,wc} M_j (C_{j,gas} - C_{j,wc}). \quad (1.4)$$

Here, w_j is the mass fraction of species j , C_j is the concentration in mole per unit volume, θ_j is the occupancy, ε_g and ε_{wc} are the volume of the gas phase respectively the washcoat per unit volume, $D_{j,eff}$ are the effective diffusion coefficients (in proper units), \dot{m} is the mass flow per unit cross section, $\nu_{j,i}$ is the stoichiometric coefficient of component j with respect to reaction i , r_i is the reaction rate for reaction i in mole per unit volume, and NC and NR are the number of components respectively reactions. The corrective summation terms for the interphase diffusion has to be included to keep the sum of mass fractions constant. A correction term for the reaction is needed as well, as the catalyst surface can store mass and therefore the sum of mass flows due to adsorption and desorption does not always vanish.

The corresponding boundary conditions are given by

$$\begin{aligned} \dot{m}_{in} w_{j,in} &= \dot{m} w_j^{gas}(0) - \varepsilon_{gas} D_{j,eff}^{gas} \frac{\partial w_j^{gas}(0)}{\partial z}, \quad \frac{\partial w_j^{gas}(L)}{\partial z} = 0 \\ \frac{\partial w_j^{wc}(0)}{\partial z} &= 0, \quad \frac{\partial w_j^{wc}(L)}{\partial z} = 0 \\ \frac{\partial \theta_j(0)}{\partial z} &= 0, \quad \frac{\partial \theta_j(L)}{\partial z} = 0, \end{aligned} \quad (1.5)$$

where L denotes the length of the reactor.

Energy Balances

For the energy balances, the model is also divided into three regions: the inner gas phase, the catalyst solid phase and the reactor wall temperature. Analog to the mass balances, transport within the gas phase is by convection and conduction, while it is purely conductive for the solid phase and wall phase. Heat transfer between the gas phase and the solid catalyst is modeled by a Nusselt number analogy, while the heat transfer from the solid catalyst to the wall is approximated as a single conduction resistance given by the insulation mat between the catalyst and the reactor wall. The transfer coefficient is determined by estimation from measurements of heat profiles obtained with non-reacting gas flows (Argon and steam). Heat capacity and conductivity of the solid catalyst are estimated from material properties of the metal carrier and the geometric structure of the monoliths. The heat-capacities and conductivity of the washcoat and the gas contained in the pores are neglected. Their capacities are small compared to the heat capacity of the metal carrier. The heat capacity of the reactor wall is also determined from the material properties of stainless steel and the geometry.

This yields the following energy balances:

Gas-phase:

$$\varepsilon_g \rho_g c_{p,g} \frac{\partial T_g}{\partial t} = \varepsilon_g \lambda_g \frac{\partial^2 T}{\partial z^2} - \dot{m} c_{p,g} \frac{\partial T}{\partial z} + \alpha_{g,s} (T_s - T_w) \quad (1.6)$$

Catalyst solid phase

$$\varepsilon_s \rho_s c_s \frac{\partial T_s}{\partial t} = \lambda_s \frac{\partial^2 T_s}{\partial z^2} - \alpha_{g,s} (T_s - T_g) - \alpha_{w,s} (T_s - T_w) + \sum_i -\Delta H_i r_i \quad (1.7)$$

Wall temperature

$$\varepsilon_w \rho_w c_w \frac{\partial T_w}{\partial t} = \lambda_w \frac{\partial^2 T_w}{\partial z^2} + \alpha_{ws} (T_s - T_w) \quad (1.8)$$

The corresponding boundary conditions are given by

$$\begin{aligned} \dot{m} c_{p,g} T_{in} &= \dot{m} c_{p,g} T_{gas}(0) - \varepsilon_g \lambda_g \frac{\partial T_{gas}(0)}{\partial z}, \quad \frac{\partial T_{gas}(L)}{\partial z} = 0 \\ \frac{\partial T_s(L)}{\partial z} &= 0, \quad \frac{\partial T_s(0)}{\partial z} = 0 \\ \frac{\partial T_w(0)}{\partial z} &= 0, \quad \frac{\partial T_w(L)}{\partial z} = 0. \end{aligned} \quad (1.9)$$

REACTION KINETICS

The reaction mechanism used in this work is shown in Table 1. The mechanism is not intended to be representing a complete set of elementary reactions. Developing and parameterizing such an elementary reaction network is not feasible for a system with the complexity of gasoline reforming. Present micro-kinetic reaction mechanisms for methane reforming consist of more than 100 reactions (6). A micro-kinetic mechanism for gasoline reforming would easily lead to a multitude thereof. Therefore, a grossly simplified reaction mechanism representing only the most important reaction steps and surface species has been selected.

Table 1: Reaction scheme

| Adsorption and Desorption reactions | | | |
|-------------------------------------|------------------------------------------------|-------------------|--------------------------------------------------------------------|
| (1) | $\text{H}_2 + 2^*$ | \leftrightarrow | 2H^* |
| (2) | $\text{O}_2 + 2^*$ | \leftrightarrow | 2O^* |
| (3) | $\text{H}_2\text{O} + 2^*$ | \leftrightarrow | $\text{H}^* + \text{OH}^*$ |
| (4) | $\text{CO} + ^*$ | \leftrightarrow | CO^* |
| (5) | $\text{Gasoline} + ^*$ | \leftrightarrow | Gasoline^* |
| (6) | $\text{C}_2\text{H}_4\text{O} + ^*$ | \leftrightarrow | $\text{C}_2\text{H}_4\text{O}^*$ |
| Reactions on the catalyst | | | |
| (7) | $\text{CO}^* + \text{O}^*$ | \leftrightarrow | $\text{CO}_2 + 2^*$ |
| (8) | $\text{H}^* + \text{O}^*$ | \leftrightarrow | $\text{OH}^* + ^*$ |
| (9) | $\text{Gasoline}^* + x_1 \text{O}^*$ | \rightarrow | $x_2 \text{C}_2\text{H}_4\text{O}^* + x_3 \text{CO}^* + x_4^*$ (1) |
| (10) | $\text{C}_2\text{H}_4\text{O}^* + \text{O}^*$ | \leftrightarrow | $2 \text{CH}^* + 2 \text{OH}^*$ |
| (11) | $\text{CH}^* + \text{O}^*$ | \leftrightarrow | $\text{CO}^* + \text{H}^*$ |
| (12) | $\text{CO}^* + \text{OH}^*$ | \leftrightarrow | $\text{CO}_2 + \text{H}^* + ^*$ |
| (13) | $\text{CH}^* + \text{OH}^*$ | \leftrightarrow | $\text{CO}^* + 2 \text{H}^*$ |
| (14) | $\text{Gasoline}^* + y_1 \text{OH}^*$ | \leftrightarrow | $y_2 \text{CH}^* + y_3 \text{H}_2\text{O} + y_4 ^*$ (1) |
| (15) | $\text{C}_2\text{H}_4\text{O}^* + \text{OH}^*$ | \leftrightarrow | $\text{CH}^* + \text{CO}^* + 2 \text{H}^* + \text{H}_2\text{O}$ |
| (16) | $\text{CH}^* + 3 \text{H}^*$ | \leftrightarrow | $\text{CH}_4 + 4^*$ |

¹the coefficients x_1 - x_4 and y_1 - y_4 depend on the actual gasoline composition. They are chosen such that the atom balance is consistent.

Reactions (1)-(6) are adsorption/desorption reactions. All surface species are assumed to adsorb onto the same reaction sites. Hydrogen and oxygen are assumed to dissociate immediately following adsorptions. Also, for water and carbon dioxide an immediate dissociation into H^* and OH^* respectively CO^* and O^* are assumed. This is done as the surface occupancies of H_2O^* and CO_2^* are very low due to the low binding energy. For the methanation reaction (16), it has been assumed that the rate limiting step is the formation of CH_2 from CH^* and H^* . The consecutive formation of CH_3 and adsorption has been assumed to be much faster and surface occupancies of CH_2 and CH_3 have been neglected. As experimental measurements show that the methane concentrations within the gasoline reformer are always below or at equilibrium, the kinetics for the adsorption of methane is not relevant in our model and the reverse rate is only needed to assure thermodynamic consistency.

Gasoline Model

It is beyond feasible limits to establish a detailed reaction network for the oxidation and steam reforming of gasoline. Therefore, in this work, gasoline is represented by a single species C_xH_y , where x and y are chosen to represent the average mole numbers of carbon and hydrogen determined from an analysis of the gasoline used. The gas phase thermodynamic data was calculated by using a combination of three typical gasoline molecules. The resulting enthalpy was adjusted such that the heating value of the total oxidation corresponds to the value determined by analysis.

In the first modeling attempts, a one step conversion of gasoline into CH^* , CO^* and OH^* according to the first equation in (1.10) was assumed. However, this leads to temperatures in excess of 1500K in the first couple of millimeters of the catalyst. Such high temperatures are not realistic and have never been observed during the measurements. In fact, at such high temperatures, the catalyst would most likely have been permanently damaged. The high temperatures result from a fast, almost total oxidation of gasoline as long as oxygen is available. One possibility to reduce the temperature in the first section is to reduce the rate of the oxidation reactions such that the energy is only gradually released. However, this leads to a penetration of oxygen far into the reactor, which contradicts the experimental results. Therefore, the gasoline oxidation was modeled via a two-step mechanism with an intermediate oxygenated hydrocarbon. The choice of C_2H_4O as oxygenated species is rather arbitrary here and should only be seen as a representative of oxygenated hydrocarbons in general. An oxygenated hydrocarbon was chosen as intermediate, as measurements indicate a significant amount of oxygenated hydrocarbon species in the product gas of an incomplete dry partial oxidation of gasoline (7).

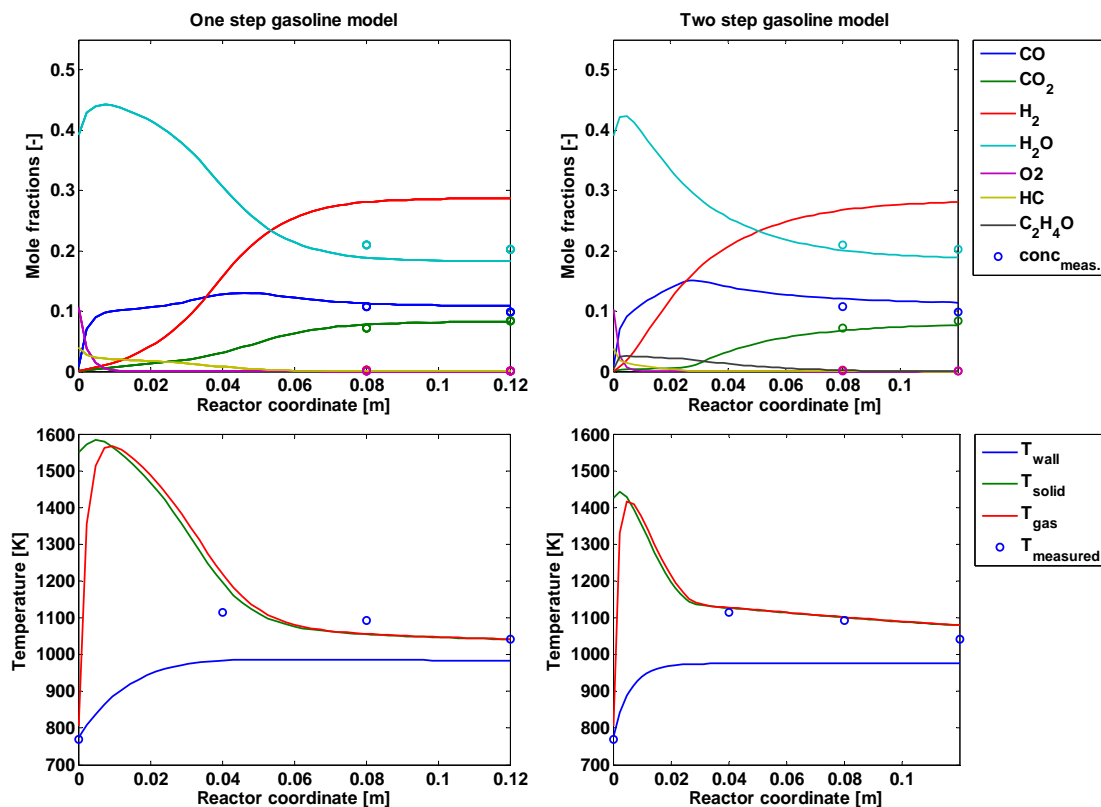
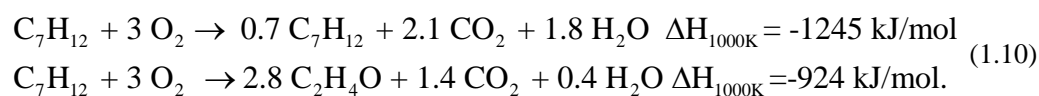


Figure 1: Comparison of mole fractions and temperatures along reactor coordinate for one-step model (left) and two-step model (right)

The two corresponding total oxidation reaction equations for the one- and two-step models at an air-to-fuel ratio of 0.3 are given by



As can be seen, the heat release due to a complete conversion of the available oxygen is about 25% lower if one assumes the formation of $\text{C}_2\text{H}_4\text{O}$ as intermediate species than in the one-step model. Therefore, the two-step mechanism results in a strong reduction of the hot spot temperatures. This is depicted in Figure 1. The input conditions are the same for both models and even though the output concentrations agree well, the temperature profile differs strongly. The two-step model shows a better agreement with measured temperatures shown as circles in Figure 1. Unfortunately, the first temperature sensor in the experimental setup is located 4 cm downstream of the catalyst bed and therefore the hot spot temperature could not be measured.

NUMERICAL SOLUTION AND PARAMETER ESTIMATION

A code generator was developed in MAPLE to implement the PDE system outlined above. The code generator reads the reaction mechanism from an xml configuration file and automatically generates optimized FORTRAN sub-routines for several PDE solvers. Currently, three solvers are supported by the code generator: PDEXPACK (8), an adaptive solver for partial differential equations with spatial discretization by second-order finite differences, BACOL (9), and BACOLR (10), both adaptive solvers based on b-spline collocation on finite elements. For the given problem, BACOL turned out to be the most efficient and robust solver.

The resulting system is computationally demanding. During fast transients, simulation speed can drop significantly below real-time. To give an approximate impression, the evaluation of a set of 27 steady states by consecutive dynamic simulation took approximately 7 minutes on a 3-GHz Pentium 4 computer. The high computational demand makes thorough parameter estimation difficult. Typically, several thousands of evaluations have to be performed resulting in run-times of days to weeks. To speed up parameter estimation, CONDOR (11) was used as optimization tool. CONDOR performs optimizations based on a trust region algorithm. It can perform simultaneous computation of the objective function on several computers, resulting in a significant speed-up. With the parallel execution on ten current workstations, the optimization process still took approximately three days.

As mentioned earlier, the heat transfer coefficients and enthalpies were estimated using experiments with pulses of steam. This allowed estimation independent of the reaction kinetics. For the further parameter estimation, it is assumed that the reaction does not change the heat transfer significantly. While there is some debate whether this is true, the influence of changing heat transfer coefficients is limited to the very first reaction zone, where oxygen is present. After this zone, the temperatures of both gas and solid phase quickly approach each other. The dynamic storage capacity of the active catalyst surface was estimated from CO sorption measurements.

The reaction rate parameters and activation energies were estimated using a set of steady state measurements obtained at our test bench. Three input parameters, mass flow of gasoline, steam-to-carbon ratio and oxygen-fuel ratio were each set to three distinct values

($P_{HC} = 1, 2, 3 \text{ kW}_{th}$, $S/C=1, 1.5, 2$, and $\lambda = 0.2, 0.3, 0.35$), resulting in a set of 27 steady-state measurements covering a wide range of operating conditions. During these measurements, the wall-temperature of the reformer was kept constant at a temperature of 973K. This was done mainly to speed up the approach to steady-state conditions during the measurement phase and to minimize the influence of heat losses of the reactor wall to the environment which are not modeled so far.

MODEL VALIDATION

Figure 2 shows the measured product mole flows vs. model results for the set of 27 steady states mentioned above. While the overall agreement is good, there are deviations for some of the measurements, especially regarding hydrogen flow. This is partly due to a high measurement uncertainty of the mass spectrometer with respect to hydrogen due to drifts. Also, the model fails to predict the conversion of hydrocarbons very well for high throughputs. Obviously, this has a strong influence on the output hydrogen mole flow. Given the simplicity of the reaction scheme, especially for the hydrocarbon oxidation and steam reforming, the observed deviations are within the expected limits.

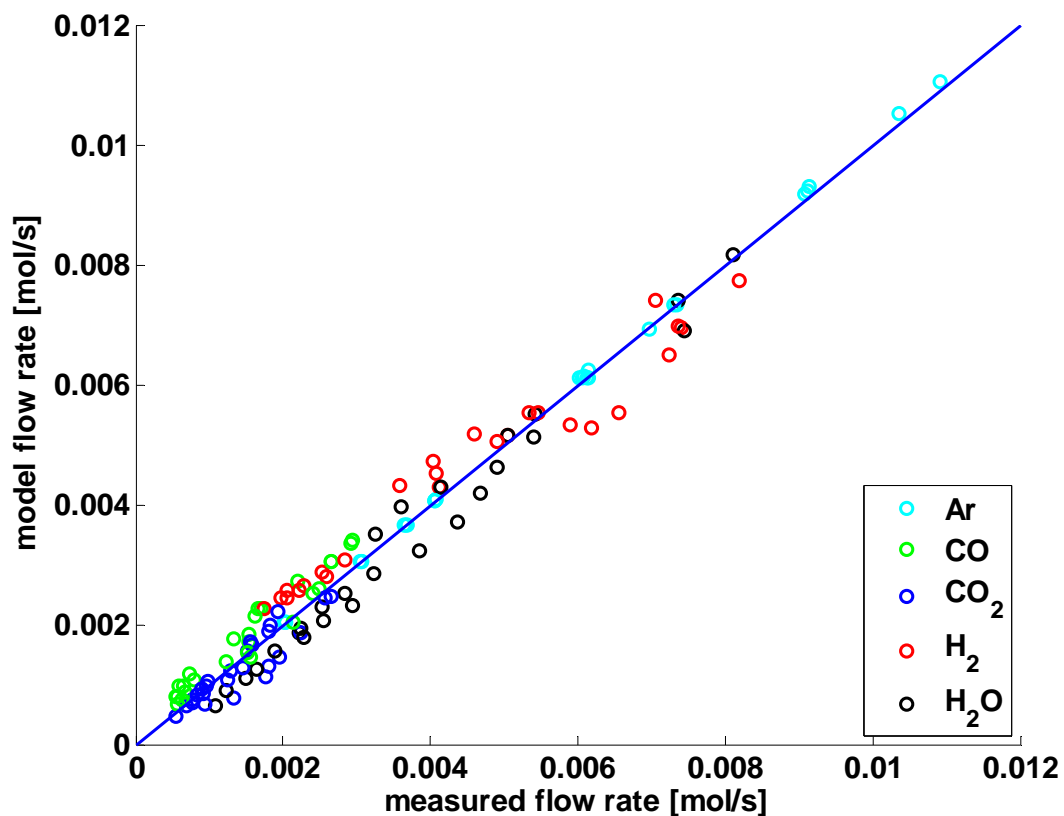


Figure 2: Steady state comparison a set of 27 operating conditions

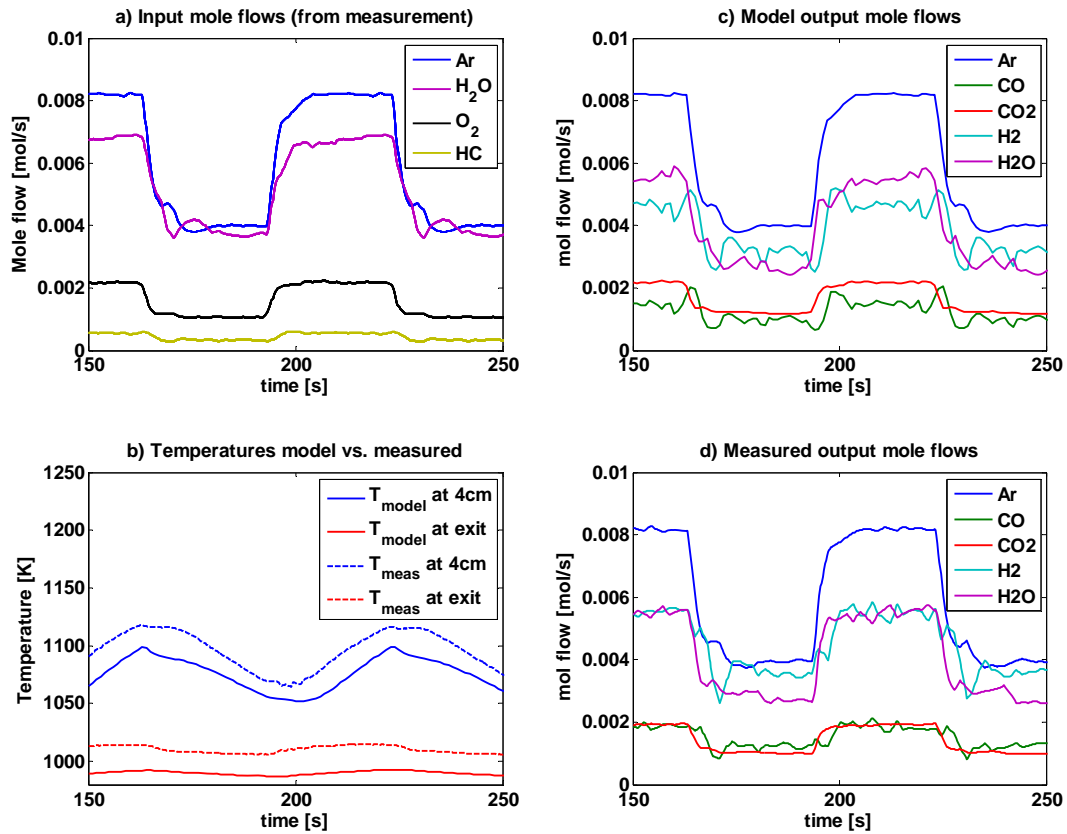


Figure 3: Measurements vs. simulation for input step changes

TRANSIENT BEHAVIOR DURING INPUT STEPS

In order to test the dynamic validity of the model, we compare the model results with step input change measurements performed on our reformer test bench. For the measurements, step input changes between 1kW_{th} and 2kW_{th} of gasoline input power have been performed. During the input steps, it was attempted to keep the input composition constant at $\lambda = 0.3$ and $S/C = 1.5$. However, due to differences in the dynamic behavior of the reactant gas supplies, especially the evaporators, constant concentrations could not be achieved. Figure 3a shows the measured mole flows at the reactor entrance over time. The mole flows were determined from measured concentrations and a mass flow measurement of the Argon input. It can be seen that the dynamics of the four reactant inputs are not equal.

As these short deviations of the input conditions during transients can have a severe impact on the output of the reformer, the simulation of the step changes was performed with the measured input mole flows as input signals. It should be noted that due to limitations of our gas sampling, the input and output concentrations could not be measured simultaneously. However, the reproducibility of the input flows was very good, so that the measurements were taken sequentially. Figure 3c and 3d show the model output and measured output mole flows. The fluctuations that can be seen are due to pulsations of the evaporators. As the measured input mole flows have been used for the model, the model also shows these fluctuations. In the measurement, during the step change to high throughput, the increase of hydrogen is delayed by approximately three seconds. During this phase, the output CO₂ flow also increases well before the CO flow follows. Both trends are captured well by the model,

although it does not completely agree on the ratio of CO and CO₂ at high flows. The temperature dynamics (Figure 3b) also shows a very good agreement. Temperatures are measured at two positions, after approx. 4 cm of reactor length and at the reactor exit. While the absolute temperatures in the model are slightly lower, the dynamics are captured well.

The results obtained during the step change measurement raise the question, whether the delay in the increase of the hydrogen mole flow is purely caused by the non-ideal behavior of the input gas streams or whether it is due to dynamic phenomena within the reformer. The simulation was therefore repeated with an ideal step change (linear increase of mass flow over 0.5s). In the ideal case, the concentrations at the input of the reactor remain constant and only the mass flow changes. The response to the ideal step changes is shown in Figure 4. In contrast to the non-ideal case, there is no significant delay in H₂ output flow. All flows follow the flow change almost instantaneous. This indicates that for an input step at these conditions, the dynamic of the catalyst surface does not influence the system significantly. Even the temperature dynamics have only little influence on the system output, causing a slight shift of the CO/CO₂ equilibrium resulting in a slightly reduced hydrogen output at high loads. It should be noted here, that the measurements and model result presented here, were all performed by keeping the reactor wall temperature at a controlled temperature. In a real reformer system, the wall temperature would also react to the changes of input flow rates. This will result in a stronger influence of the temperature dynamics on the output flows.

The fact that the ideal input step simulation shows an almost instantaneous reaction to the input changes also indicates that the delays in hydrogen flow observed in the measurements is purely caused by the imperfection of the feed supply. This emphasizes the need for precise control of input gas streams as even small deviations can have a pronounced effect on output gas streams.

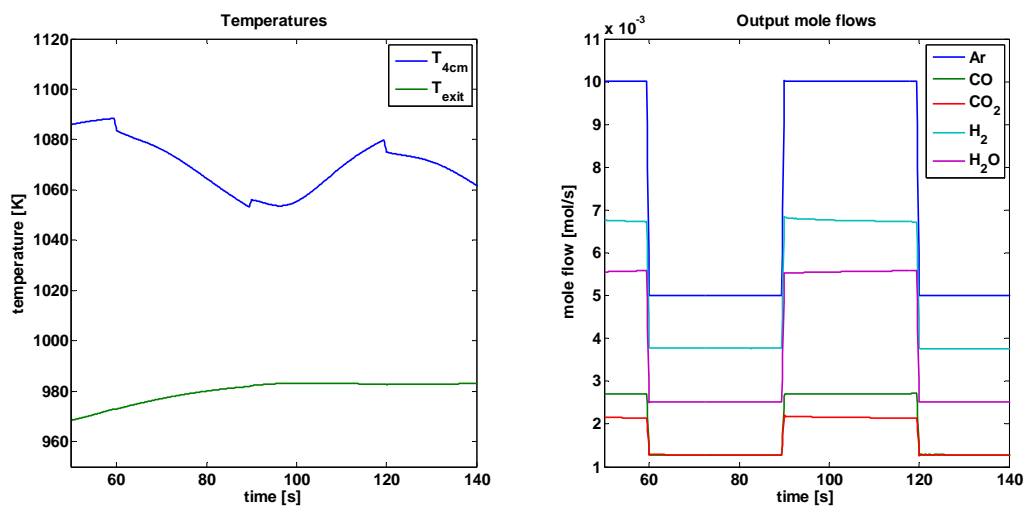


Figure 4: Simulation of ideal input steps

CONCLUSIONS

A dynamical model of a gasoline reformer was presented. It was shown, that a one-step gasoline oxidation model leads to excessive temperatures not observed in measurements. Therefore, a two-step model via an oxygenated hydrocarbon species was proposed. Albeit the gross simplification of the gasoline oxidation and reforming pathway, the presented model is able to reproduce steady state measurements over a large variation of input conditions. Also,

the dynamic response during input steps is well captured. Using the simulation of an ideal input step, it was shown that the delay in hydrogen outflow observed in measurements is likely due to a non-ideal behavior of the reactant supply system. This indicates the importance of a precise control of input gas concentration during transient operation. The ideal simulation also revealed no significant influence of the catalyst surface dynamics on the output of the reformer; however, given the simplicity of the reaction mechanism, this proposition should be dealt with great care.

ACKNOWLEDGEMENTS

We would like to thank the Catalytic Process Engineering group at the Paul Scherrer Institute, PSI, for many valuable discussions and helpful advice, and for providing the space and infrastructure for operating our test bench.

REFERENCES

- (1) S. Springmann, M. Bohnet, M. Sommer, M. Himmen, and G. Eigenberger, "Steady-state and Dynamic Simulation of an Autothermal Gasoline Reformer," *Chemical Engineering & Technology*, vol. 26, pp. 790-796, 2003.
- (2) D. Papadias and D. J. Chmielewski, "Autothermal Reforming of Gasoline for Fuel Cell Applications: A Transient Reactor Model," *Ind. Eng. Chem. Res.*, submitted for publication.
- (3) M. Pacheco, J. Sira, and J. Kopasz, "Reaction kinetics and reactor modeling for fuel processing of liquid hydrocarbons to produce hydrogen: isooctane reforming," *Applied Catalysis A: General*, vol. 250, pp. 161-175, 2003.
- (4) T. S. Auckenthaler, C. H. Onder, H. P. Geering, and J. Frauhammer, "Modeling of a three-way catalytic converter with respect to fast transients lambda-sensor relevant exhaust gas components," *Industrial & Engineering Chemistry Research*, vol. 43, pp. 4780-4788, 2004.
- (5) R. E. Hayes and S. T. Kolaczkowski, "A study of Nusselt and Sherwood numbers in a monolith reactor," *Catalysis Today*, vol. 47, pp. 295-303, 1999.
- (6) A. B. Mhadeshwar and D. G. Vlachos, "Hierarchical multiscale mechanism development for methane partial oxidation and reforming and for thermal decomposition of oxygenates on Rh," *Journal of Physical Chemistry B*, vol. 109, pp. 16819-16835, 2005.
- (7) M. Bosco, "Personal Communication," Paul Scherrer Institute, 2006.
- (8) U. Nowak, J. Frauhammer, and U. Nieken, "A fully adaptive algorithm for parabolic partial differential equations in one space dimension," *Computers & Chemical Engineering*, vol. 20, pp. 547-561, 1996.
- (9) R. Wang, P. Keast, and P. Muir, "BACOL: B-spline adaptive COLlocation software for 1-D parabolic PDEs," *Acm Transactions on Mathematical Software*, vol. 30, pp. 454-470, 2004.
- (10) R. Wang, P. Keast, and P. H. Muir, "Collocation software based on Runge-Kutta time integrator for 1-D parabolic PDEs and Schrodinger type problems, with spatial and temporal error control," Saint Mary's University Department of Mathematics and Computing Science Technical Report 2005-003, 2005.
- (11) F. Vanden Berghen and H. Bersini, "CONDOR, a new parallel, constrained extension of Powell's UOBYQA algorithm: Experimental results and comparison with the DFO algorithm," *Journal of Computational and Applied Mathematics*, vol. 181, pp. 157-175, 2005.